Deep-Sea Research, Vol. 34, No. 1, pp. 123–137, 1987.
Printed in Great Britain.

0198–0149/87 $3.00 + 0.00
© 1987 Pergamon Journals Ltd.

Nonlinear effects in the seasonal cycle of the tropical Atlantic Ocean

S. G. H. PHILANDER* and R. C. PACANOWSKI*

(*Received* 17 *January* 1986; *in revised form* 22 *May* 1986; *accepted* 10 *June* 1986)

Abstract—Nonlinearities have a large effect on the circulation of the tropical Atlantic Ocean within a few hundred kilometers of the equator, both in the surface layers and at depth. Qualitative features of a nonlinear model that are absent from a linear model include energetic unstable waves in the western equatorial Atlantic and a westward surface jet that penetrates to considerable depths between the equator and 3°N. The largest quantitative difference between the nonlinear and linear models is the intensity of the westward surface flow at the equator. In a linear model it can be twice as fast as in a nonlinear model. Motion below the equatorial thermocline, though sufficiently slow to be linear, is related to the surface forcing in a nonlinear manner because it is forced to a large extent by vertical movements of the thermocline. (Linear models assume that disturbances reach the deep ocean by propagating through a fixed thermocline.) In addition to the equatorial zone, nonlinearities affect the coastal zone of Africa south of the equator, where alongshore currents and zonal pressure gradients in linear and nonlinear models are different.

INTRODUCTION

A SCALE-ANALYSIS based on the observed intensity and width of equatorial currents reveals that the nonlinear terms in the equations of motion are important near the equator. A number of studies have explored the effects of nonlinearities in idealized situations. In general, nonlinearities intensify eastward equatorial currents and weaken westward currents. In the case of the eastward flowing Equatorial Undercurrent, the intensification is associated with vorticity conservation by fluid elements that travel equatorward in the thermocline (FOFONOFF and MONTGOMERY, 1966; CHARNEY, 1960; ROBINSON, 1966). In the case of eastward equatorial surface jets driven by eastward winds, intensification is caused by equatorward Ekman drift which advects eastward momentum, gained from the wind, towards the equator. Westward winds, on the other hand, drive poleward Ekman drift (which disperses the zonal momentum) and cause equatorial upwelling (of water with low zonal momentum) so that the westward equatorial jet is weaker in the nonlinear than linear case (CANE, 1979, 1980; PHILANDER, 1979).

As yet there has been no attempt to assess the role of nonlinearities in a realistic simulation of the circulation of a tropical ocean. Several investigators have forced relatively simple linear models with realistic climatological winds and have succeeded in reproducing some of the features of the observed seasonal cycle (BUSALACCHI and PICAUT, 1983; DU PENHOAT and TRÉGUIER, 1985). The nonlinearities, however, are not

* Geophysical Fluid Dynamics Laboratory/NOAA, Princeton University, Princeton, NJ 08542, U.S.A.

negligible so that these calculations are inconsistent. How will the results be modified if the nonlinearities are taken into account? This paper addresses this question by using a multi-level high resolution general circulation model that simulates the seasonal cycle in the tropical Atlantic Ocean realistically. KATZ (1984), GARZOLI and PHILANDER (1985). and RICHARDSON and PHILANDER (1986) compare results from the model with measurements. Here we compare results from linear and nonlinear versions of the model. For a more detailed discussion of the nonlinear simulation the reader is referred to PHILANDER and PACANOWSKI (1986).

THE MODEL

The Atlantic Ocean model extends from 28°S to 50°N latitude. The longitudinal resolution is a constant 100 km, with a latitudinal resolution of 33 km between 10°S and 10°N, increasing gradually poleward of this region. At 25°N the latitudinal spacing is 200 km. The topography of the ocean floor is taken into account, except that islands are 150 m below the sea surface and the coastal shelf is 50 m below the sea surface. There are 27 levels in the vertical; the upper 100 m have a resolution of 10 m.

The primitive equations are solved numerically by means of finite differencing methods discussed in BRYAN (1969). The use of Richardson number dependent vertical mixing coefficients is explained in detail in PACANOWSKI and PHILANDER (1981). In the upper 10 m of the model the coefficient of vertical eddy viscosity has a minium value of 10 $cm^2\ s^{-1}$ to compensate for mixing by the high frequency wind fluctuations which are absent from the monthly mean winds. In the deep ocean, where vertical mixing is negligible, vertical viscosity has the value of molecular viscosity. The coefficients of horizontal eddy viscosity and diffusivity are 2×10^7 $cm^2\ s^{-1}$ equatorward of 10° latitude; poleward of this they increase gradually to a value of 50×10^7 $cm^2\ s^{-1}$ at 50°N. Unstable temperature gradients are eliminated instantaneously by mixing heat vertically to a depth that ensures a stable temperature gradient.

Poleward of 20°S and 30°N the equation for temperature T gains a term $\gamma(T-T^*)$, where T^* is the prescribed monthly mean climatological temperature for the region under consideration, and γ is a Newtonian cooling coefficient. Its value is 1/(2 days) near the zonal boundaries and decreases to a value of zero equatorward of 30°N and 20°S. This device mitigates the effect of the artifical zonal walls along the southern and northern boundaries of the ocean and forces the solution towards the climatology in these regions.

The heat flux across the ocean surface is

$$Q = SW - LW - QS - QE.$$

The solar short wave heating, SW, is taken to be 500 ly day^{-1} equatorward of 20° latitude and to decrease linearly to 300 ly day^{-1} between 20° and 45° latitude. The long wave back radiation, LW, has a constant value of 115 ly day^{-1}. The sensible heat flux is

$$QS = \rho C_D C_P V(T_0 - T_A)$$

and the evaporation is

$$QE = \rho C_D L V[e_s(T_0) - \alpha\, e_s(T_A)](0.622/p_A),$$

where the saturation vapour temperature is

$$e_s(T) = 10^{(9.4-(2353/T))}.$$

Here $\rho = 1.2 \times 10^{-3}$ g cm^{-3}; $L = 595$ cal g^{-1}; $C_D = 1.4 \times 10^{-3}$; $p = 1013$ mb; $C_p = 0.24$ cal g^{-1} °C^{-1}; T_0 is the sea surface temperature in °K; T_A is the atmospheric temperature at the surface; V is the surface wind speed; and the relative humidity α is assigned the constant value 0.8. No provision is made for clouds. The sensible heat flux is found to be of secondary importance so that variations in heat flux are primarily a consequence of change in the evaporation. Since evaporation depends on the wind speed, avoidance of excessively high temperature in regions of weak winds requires that the wind speed not be <3.5 m s^{-1}. This minimum parameterizes evaporation caused by high-frequency wind fluctuations that are absent from the mean monthly winds. This restriction applies only to the evaporative term.

The initial conditions for the model are zero currents and the climatological temperature field of January (LEVITUS, 1982). Monthly averaged climatological winds (HELLERMAN and ROSENSTEIN, 1983) then force the model for 2 years by which time the model has an equilibrium seasonal cycle. The results shown here are from the third year of the simulation.

In the linear version of the model the equations of motion are linearized about a state of no motion in which the basic stratification is independent of horizontal position and is a spatial average of the January stratification along the equator in the LEVITUS (1982) data. This is an arbitrary choice for the basic stratification, but given the considerable spatial and temporal variations of the thermal structure, it is no more arbitrary than some other choice. What is important is that it captures the main feature of the thermal structure, namely the sharp, shallow thermocline. The linear version of the model retains the following nonlinear features: the nonlinear heat flux condition at the surface, the mixing parameterization, and the convective adjustment in the case of unstable temperature gradients.

RESULTS

Seasonal changes in surface winds over the tropical Atlantic are largely associated with the meridional movements of the Intertropical Convergence Zone (ITCZ) onto which the southeast and northeast trade winds converge. When the ITCZ is close to the equator, in March and April, the southeast trades are weak and winds near the equator are relaxed. In September and October the ITCZ is furthest from the equator and the southeast trades, which cross the equator, are most intense. The oceanic response to the winds is particularly dramatic during the months when the winds intensify. When the winds are weak, in March and April, thermal gradients are at a minimum and the surface flow is predominantly westward and weak except for the Brazilian Coastal Current which flows towards the Gulf of Mexico. The intensification of the trades from May onwards causes a separation of the Brazilian Coastal Current from the coast near 5°N, and the appearance of an intense eastward North Equatoral Countercurrent between 3° and 10°N approximately. The linear version of the model qualitatively reproduces these features (Fig. 1) and also the associated changes in the thermal structure, especially the trough of the thermocline along 3°N (Fig. 2). There are discrepancies in the intensities of the currents and in the magnitude of the density gradients (to be discussed in more detail shortly), but the linear model succeeds in simulating the major changes in the oceanic circulation caused by the intensification of the winds.

The variable for which there is the least difference between the linear and nonlinear models is the vertical integral of the temperature (Fig. 3) which is related to the dynamic

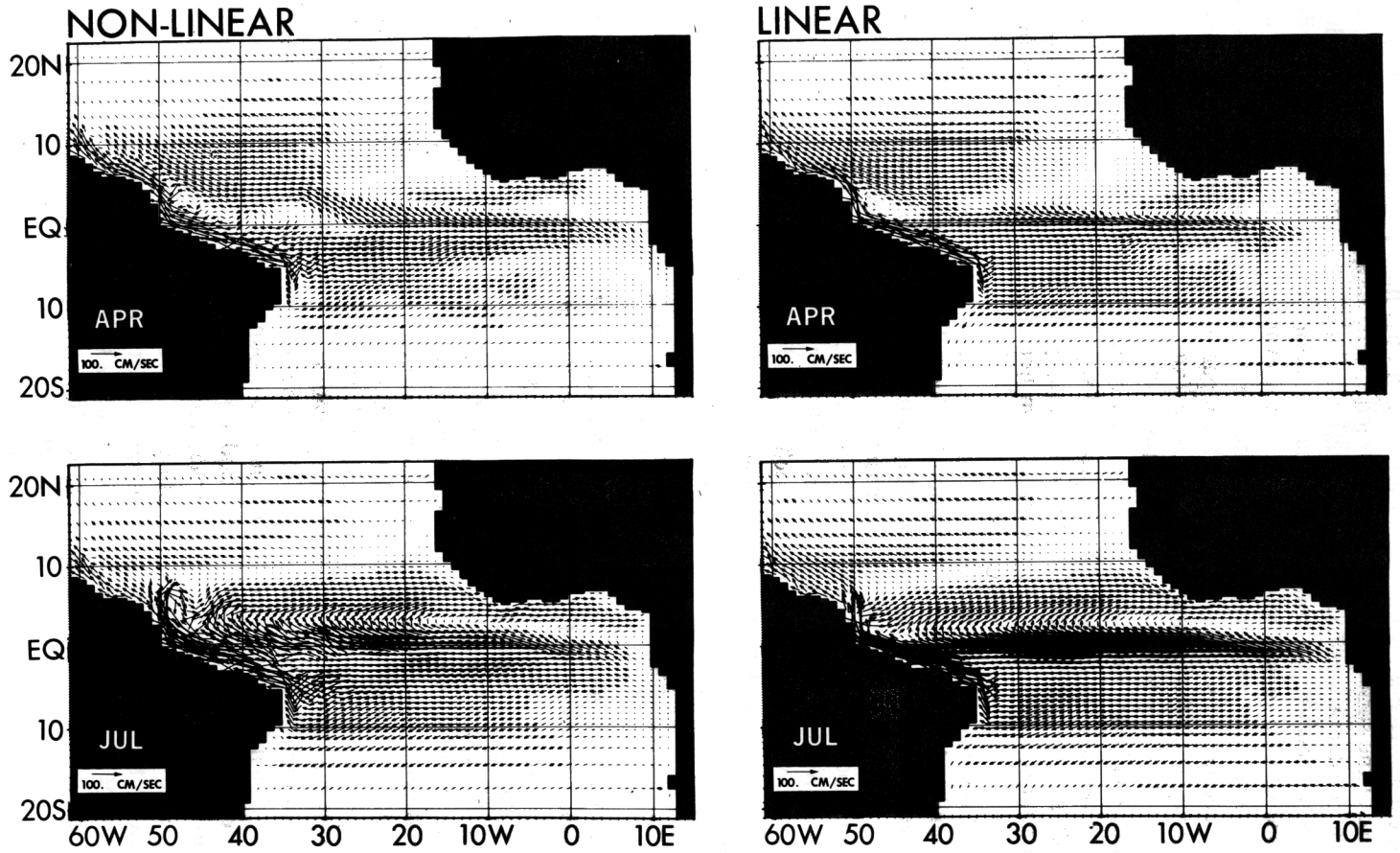

Fig. 1. Horizontal current vectors at the ocean surface on 15 April and 15 July in linear and nonlinear models.

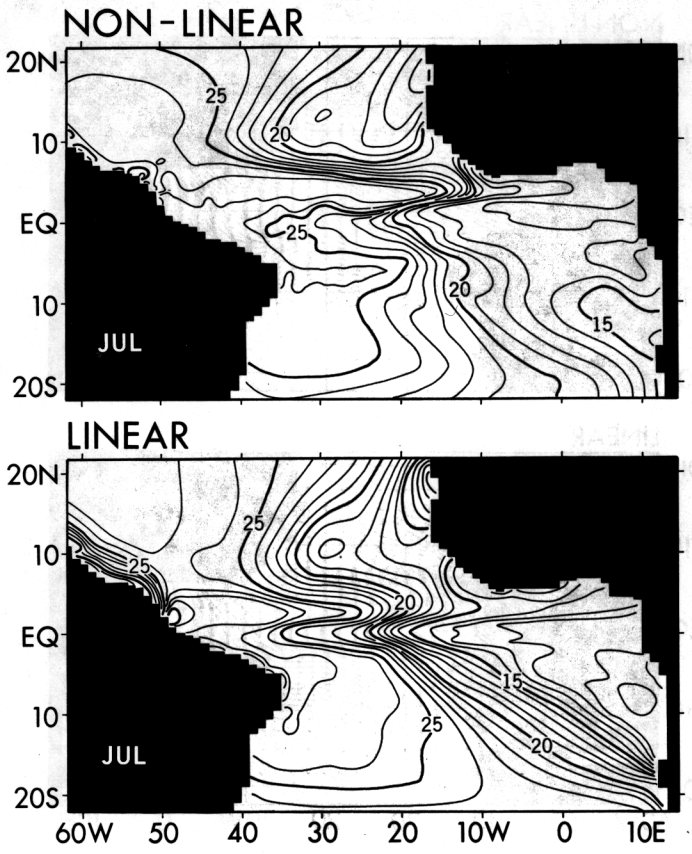

Fig. 2. Temperature in °C at a depth of 55 m on 15 July in linear and nonlinear models.

topography. The annual harmonic of this variable shows a sharp change in phase across 8°N approximately in the western side of the ocean basin. The annual harmonic of the curl of the wind has a similar structure which suggests that Ekman suction contributes significantly to this feature (GARZOLI and KATZ, 1983).

Figure 4 depicts seasonal changes, along the equator, of the surface currents and vertical integral of the temperature, in the linear and nonlinear models. Variations in the vertical integral of the temperature in the two models are again in reasonably good agreement. An interesting difference is the westward displacement of the upwelling of the Gulf of Guinea in the nonlinear model. (The minimum of the integrated temperature in June and July is further west in the nonlinear than in the linear model.) This feature reflects the more intense response of the nonlinear model to the eastward winds that prevail east of the Greenwich meridian. These winds have their largest zonal extent in October when the nonlinear (but not the linear) model has isotherms that slope downwards to the east near the African continent (Fig. 5). This figure also shows that although the vertical integral of the temperature may be similar in the two models, the depth of a specific isotherm can be very different. The linear assumption, that tempera-

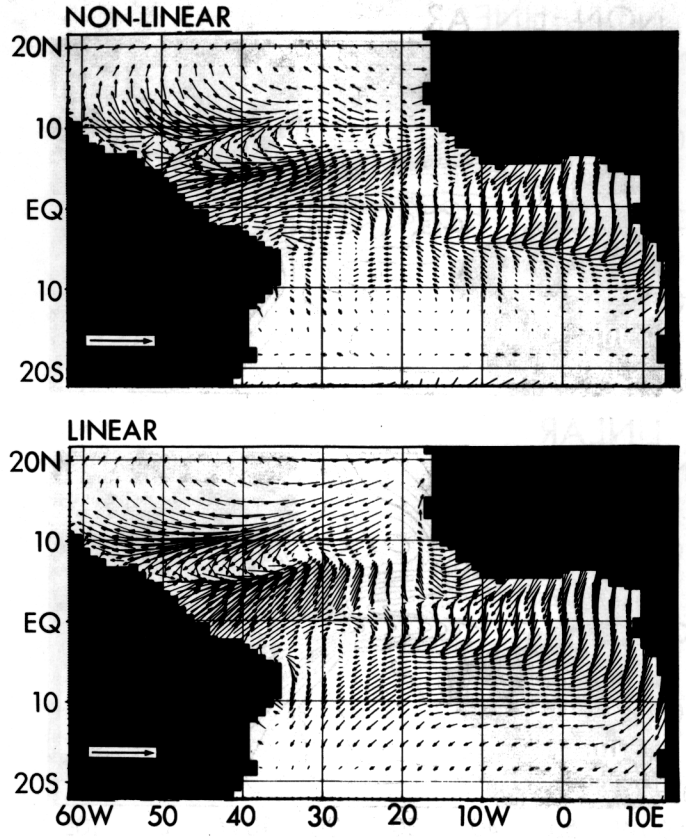

Fig. 3. The annual harmonic of the vertically averaged temperature of the upper ocean in a linear and nonlinear model. The vertical integral is taken between the surface and 317 m. The length of an arrow measures the amplitude, the direction of the arrow measures the phase. The phase increases in a clockwise sense and is 1 January for an arrow that points downwards, 1 June for an arrow that points upwards. The length of the reference arrow (in Brazil) corresponds to an amplitude of 50×10^3 cal cm $^{-2}$.

ture variations are small perturbations to a stratification which is independent of horizontal position, is seen to be invalid.

Discrepancies between the surface currents along the equator in the linear and nonlinear models are enormous (Fig. 6). The maximum westward speed in the linear case is almost twice the maximum speed in the nonlinear case. The upwelling of eastward momentum, from the Equatorial Undercurrent into the surface layers is principally responsible for this difference. Another factor is the instability which is excited in the nonlinear (but not linear) model when the shear between the westward South Equatorial Current and the neighboring eastward North Equatorial Countercurrent becomes large. The instability reduces the shear, and hence the intensity of the westward flow, and gives rise to westward traveling waves with a period of 3 weeks approximately and a wavelength near 1000 km. The waves are evident in Fig. 4.

The differences between the linear and nonlinear Equatorial Undercurrents are smaller than those between the surface currents (Fig. 6). This does not imply that

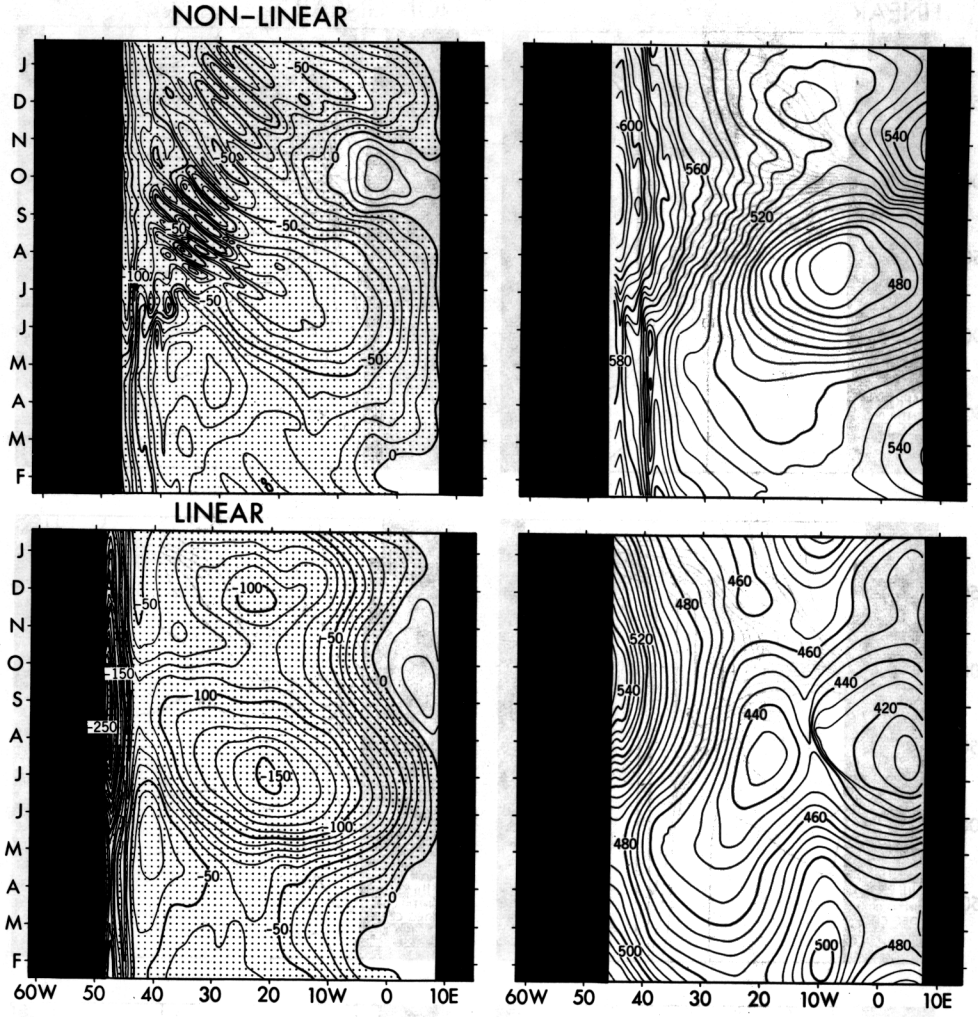

Fig. 4. Variations along the equator, as a function of time, for the zonal component of the surface current in cm s^{-1} on the left (regions of westward flow are shaded) and for the vertically averaged temperature of the upper ocean between the surface and 317 m in units of 10^3 cal cm^{-2} on the right.

nonlinearities are unimportant in the Undercurrent. The meridional flow that converges on the Undercurrent tends to conserve the vertical component of its vorticity (in a nonlinear model) and this accelerates the Undercurrent eastward (FOFONOFF and MONTGOMERY, 1955). This eastward momentum is transferred to the surface layers by equatorial upwelling (induced by the westward winds) so that linear and nonlinear models are in better agreement at the depth of the Undercurrent than in the surface layers. In the west, where an annual harmonic is dominant, the considerable vertical movements of the core of the Undercurrent are similar in the two models: the Undercurrent is shallow in April and May and deep in September. The maximum speed of the Undercurrent is somewhat less in the linear than nonlinear model. In the Gulf of

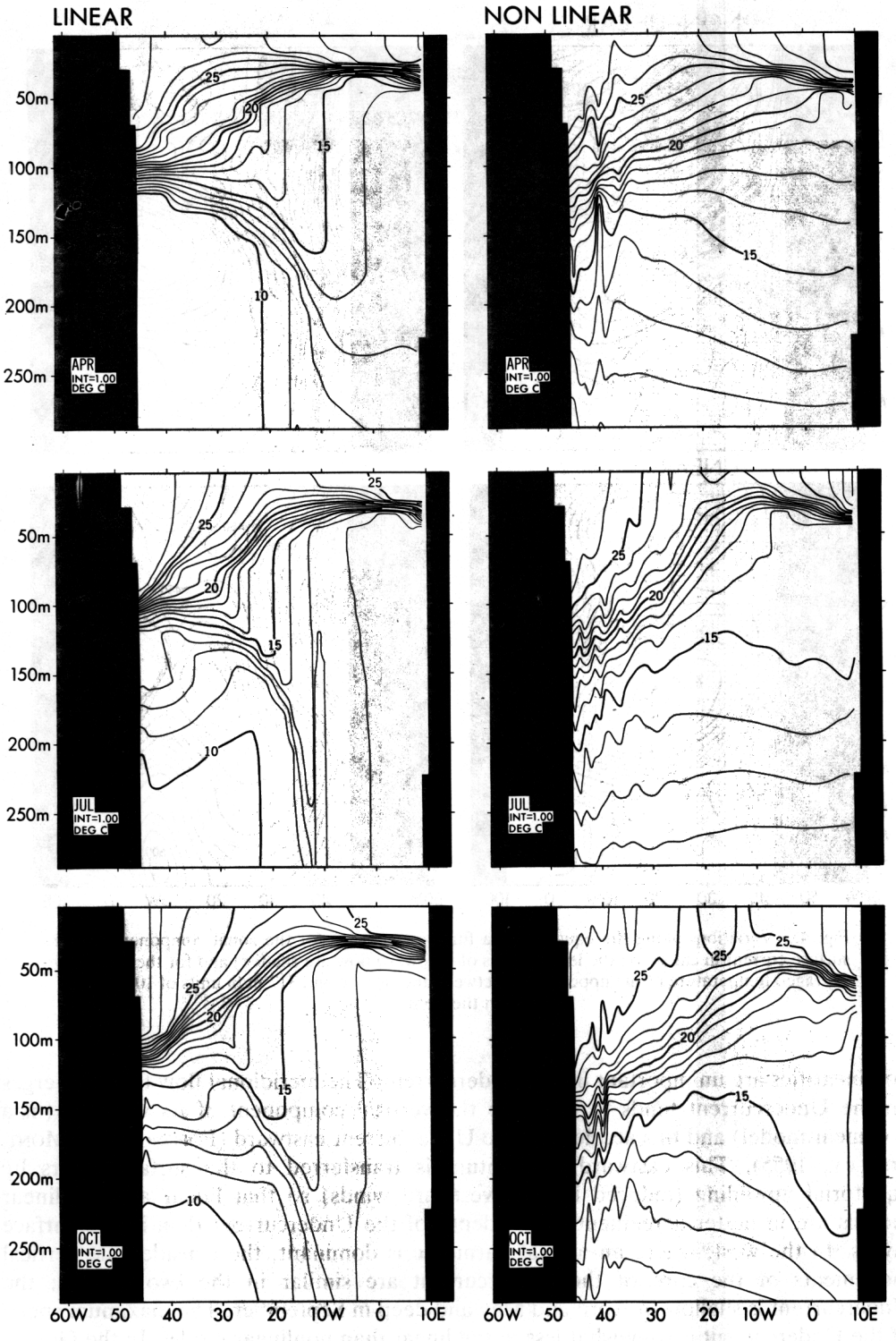

Fig. 5. Sections of the temperature in °C along the equator on 15 April, 15 July and 15 October for the linear and nonlinear cases.

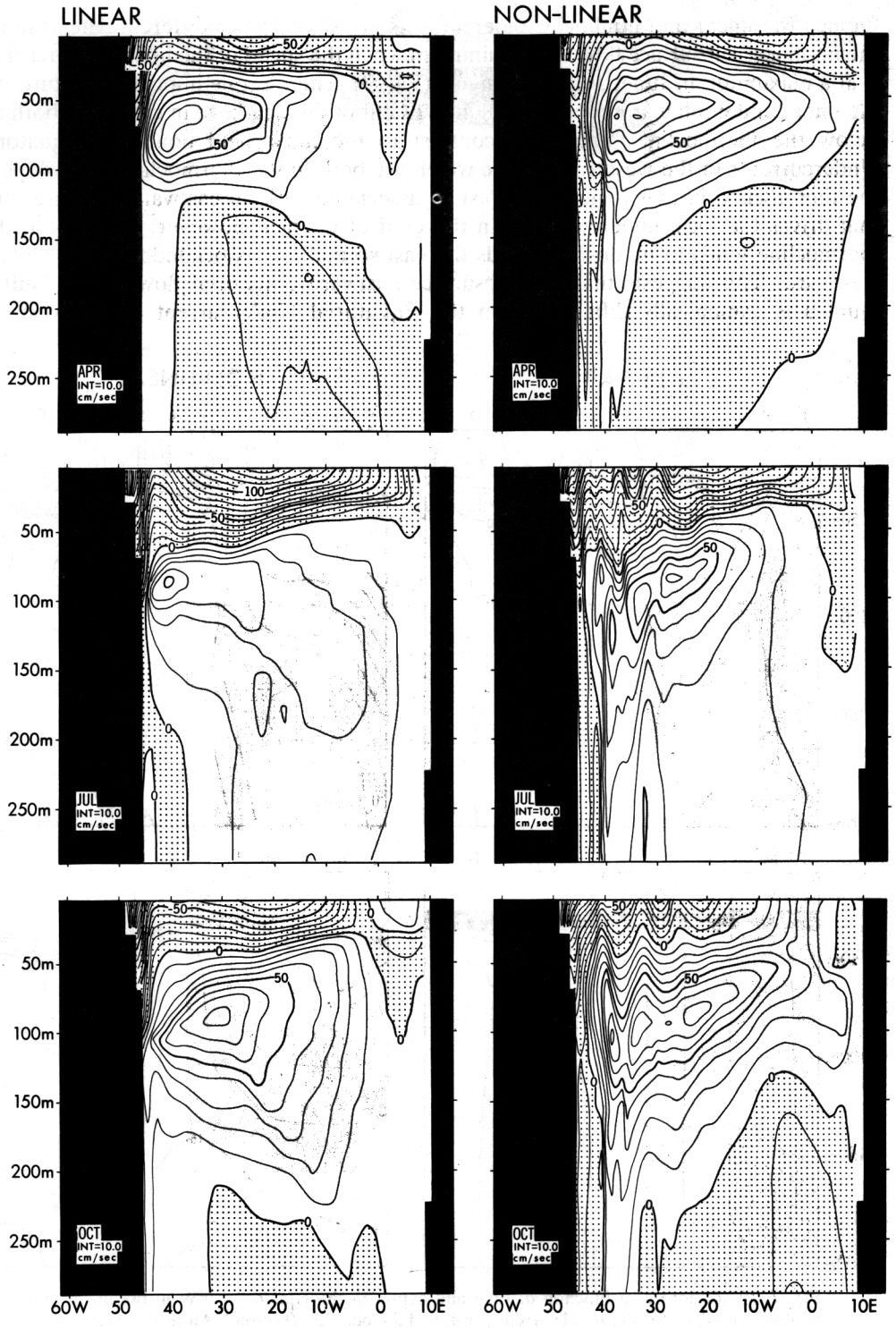

Fig. 6. Sections of the zonal velocity component along the equator (cm s^{-1}; westward flow in shaded areas) on 15 April, 15 July and 15 October in the linear and nonlinear model.

Guinea the linear and nonlinear undercurrents are significantly different: the speed of the nonlinear subsurface flow is at a minimum when the speed of the linear undercurrent is at a maximum, in June, July and August (Fig. 7). There is one important feature that the linear and nonlinear undercurrents in the Gulf of Guinea have in common: both are below the thermocline. This is in contrast to the linear and nonlinear Equatorial Undercurrents in the western Atlantic which are both *in* the thermocline. The slope of the thermocline in that region, the west, is associated with an eastward pressure force that drives the local undercurrents. In the Gulf of Guinea, however, the slope of the thermocline tends to be down towards the east so that the associated pressure force is westward. This suggests that the subsurface eastward equatorial flow in the Gulf of Guinea is dynamically different from the Equatorial Undercurrent in the west. To

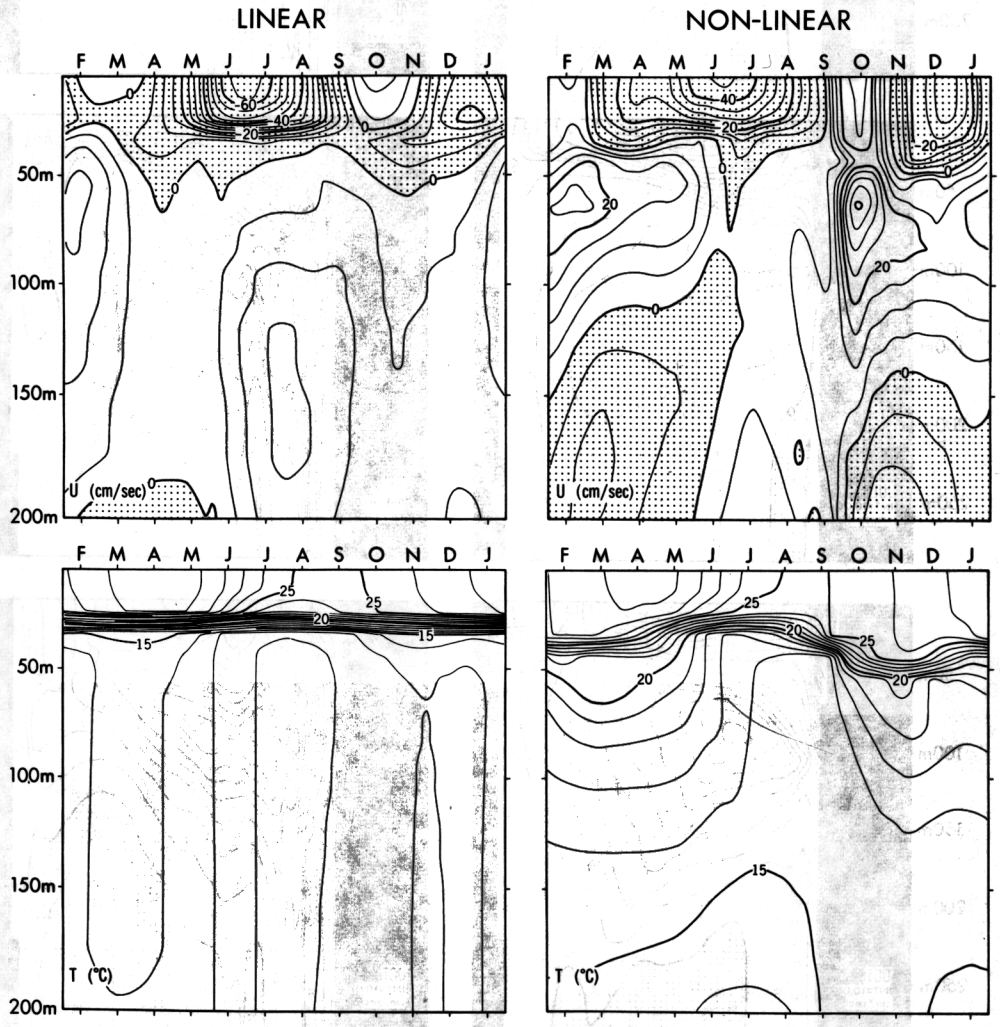

Fig. 7. Variations as a function of time and depth on the equator at 0°W in the linear and nonlinear models, for the zonal current (top), and temperature (bottom). Motion is westward in shaded areas.

explain the deep flow in the Gulf of Guinea it is necessary to explain how the currents below the thermocline are related to the surface winds. In a linear model motion is assumed to correspond to small perturbations to a state in which the ocean is at rest, while the stratification is independent of horizontal position and time. Disturbances therefore arrive below the thermocline by propagating through the fixed thermocline. A strong thermocline, such as that in the tropics, therefore could inhibit the deep penetration of disturbances (because of internal reflections in the thermocline, for example). In reality, and in the nonlinear model, these arguments are of limited relevance because the thermocline itself heaves up and down with a large amplitude, thus directly forcing motion in the deep ocean. The motion below the thermocline may be sufficiently slow to be linear, but that motion cannot be related to the surface forcing in a

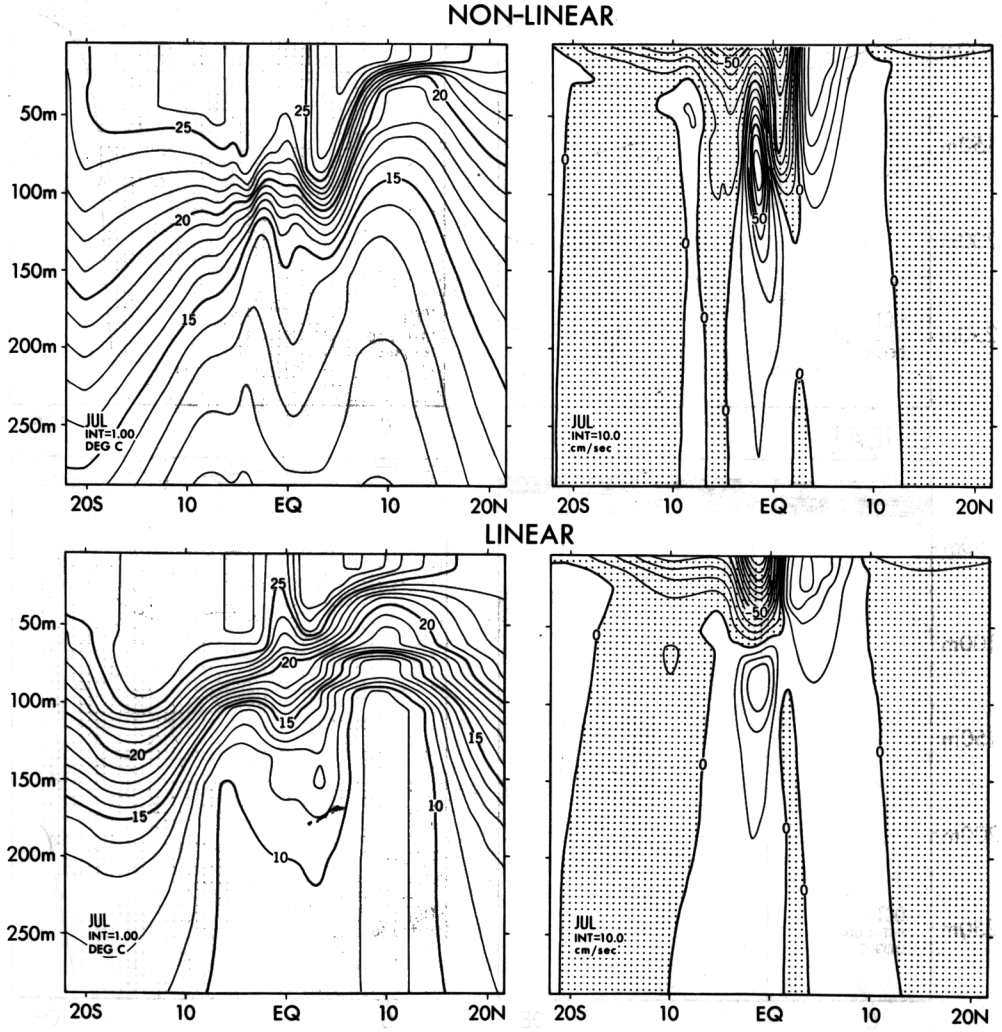

Fig. 8. Latitudinal sections on 15 July along 30°W in the linear and nonlinear models for the zonal velocity component and temperature. Motion is westward regions. The contour intervals are 1°C and 10 cm s^{-1}.

linear manner. The differences between the subthermocline currents in Fig. 7 provide a measure of the importance of nonlinearities.

The northward component of the southeast trades drives westward Ekman drift to the south of the equator and eastward Ekman drift north of the equator. In a nonlinear model the westward flow is advected into the northern hemisphere. The northward winds also induce downwelling near 3°N (a radius of deformation from the equator) so that the

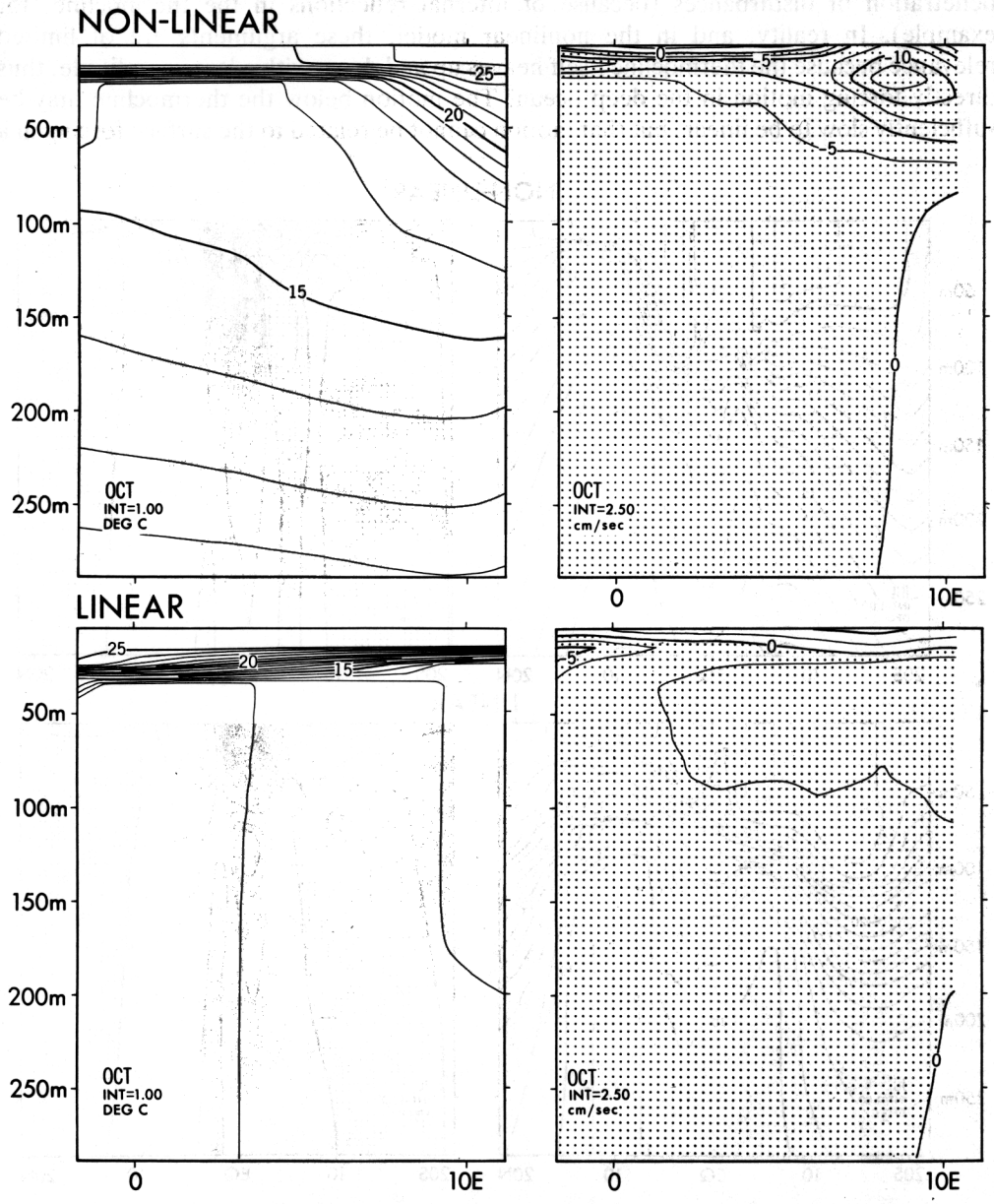

Fig. 9. The temperature (left) and meridional current (right) along 5°S near the African coast in the linear and nonlinear models. Motion is southward in shaded areas. The contour intervals are 1°C and 2.5 cm s^{-1}.

westward flow north of the equator penetrates to considerable depths in a nonlinear but not linear model. These various features are evident in Fig. 8, which shows sections along 30°W on 15 July when the southeast trades are intense. Not only the northward component of the wind but also the latitudinal shear of the westward wind contribute to the asymmetry about the equator; both contribute to the downwelling near 3°N. The southward displacement of the core of the Equatorial Undercurrent in the nonlinear model is in part attributable to advection by southward motion driven by a southward pressure force maintained by the northward winds (CHARNEY and SPIEGEL, 1971). (Because of instabilities mentioned earlier the Undercurrent meanders about the equator and is not always as far south as in Fig. 8.) The eastward North Equatorial Countercurrent is quite similar in the two models even though the associated thermal structures have large differences.

In the Gulf of Guinea, winds within a few hundred kilometers of the African coast have an eastward component. As mentioned in the Introduction, nonlinearities intensify the response of the equatorial zone to eastward winds. This is evident in Figs 5 and 6, especially in October when the downward slope (to the east) of the thermocline is far more pronounced in the nonlinear than linear model. This difference is not confined to the equatorial zone but extends from the northern coast (near 5°N) to 10°S at least. The slope of the thermocline is associated with a westward pressure force which drives a westward coastal undercurrent near 5°N. Along 5°S the slope of the thermocline is balanced by a geostrophic southward current. Both the slope and the current are absent from the linear model (Fig. 9). Between October and February this coastal current gradually disperses westward. The nonlinearities therefore affect a wide coastal zone to the south of the equator in the Gulf of Guinea. The differences between the linear and nonlinear currents to the north of the equator in the Gulf of Guinea are relatively small.

CONCLUSION

The effect of nonlinearities on the circulation of the tropical Atlantic Ocean is most pronounced within a few hundred kilometers of the equator and results in qualitative and quantitative differences between linear and nonlinear models. Qualitative features of a nonlinear model that are absent from a linear model include energetic unstable waves in the western equatorial Atlantic, a westward jet that penetrates to a considerable depth between the equator and 3°N in the western side of the basin, and a downward slope of isotherms towards the African coast near 10°E where the winds are eastward. The largest quantitative difference between the linear and nonlinear models is in the intensity of the westward surface flow at the equator. Upwelling of eastward momentum from the Equatorial Undercurrent makes the surface flow much weaker in the nonlinear than linear case.

The variable that is least affected by nonlinearities is the vertical integral of the temperature, a measure of the dynamic topography. This is so even though the temperature at a given depth is significantly different in the linear and nonlinear models. It is as if nonlinearities redistribute properties in the vertical so that the vertical integrals minimize their effect. It is tempting to infer from this result that motion in the deep ocean, where currents are sufficiently slow for the flow to be linear, is linearly related to the surface forcing even though there is a highly nonlinear surface layer. The results

shown here (e.g. Fig. 7) suggest otherwise. Motion below the thermocline, although probably linear, is very different in the linear and nonlinear models. In a linear model disturbances reach the deep ocean by propagating through the specified fixed thermocline. In the nonlinear model the vertical movements of the thermocline directly force the deep ocean.

The results indicate that certain phenomena cannot be explained strictly in terms of linear theory. An example is the motion below the equatorial thermocline where zonal jets are observed (LUYTEN and SWALLOW, 1976; ERIKSEN, 1981). The manner in which the jets derive their energy from the surface winds has been a subject of much discussion (GENT and LUYTEN, 1985). The results presented here show that the nonlinear response of the upper ocean significantly affects the motion below the thermocline. Another region affected by nonlinearities is the coastal zone of Africa south of the equator, where southward current appears in the nonlinear but not in the linear model (Fig. 9). Linear models do succeed in capturing the essence of many aspects of the seasonal cycle, such as changes in the dynamic topography. It is therefore justified to use linear models for the development of predictive schemes for sea level (INOUE and O'BRIEN, 1984). Sea surface temperature, because it is influenced by advection, is a nonlinear parameter. However, it is possible to modify linear models in a relatively simple manner in order to cope with this parameter (SCHOPF and CANE, 1983). Such modified linear models are powerful tools for the study of air–sea interactions (CANE and ZEBIAK, 1985).

Acknowledgement—We are indebted to Joan Pege and Philip Tunison and his staff for technical assistance in the preparation of this paper.

REFERENCES

BRYAN K. (1969) A numerical method for the study of the world ocean. *Journal of Comparative Physiology*, **4**, 347–376.

BUSALACCHI A. J. and J. PICAUT (1983) Seasonal variability from a model of the tropical Atlantic Ocean. *Journal of Physical Oceanography*, **13**, 1564–1588.

CANE M. A. (1979) The response of an equatorial ocean to simple windstress patterns: II. Numerical results. *Journal of Marine Research*, **37**, 253–299.

CANE M. A. (1980) On the dynamics of equatorial currents with application to the Indian Ocean. *Deep-Sea Research*, **27**, 525–544.

CANE M. A. and S. E. ZEBIAK (1985) A theory for El Niño and the Southern Oscillation. *Science*, **228**, 1085–1087.

CHARNEY J. G. (1960) Non-linear theory of a wind-driven homogeneous layer near the equator. *Deep-Sea Research*, **6**, 303–310.

CHARNEY J. G. and S. L. SPIEGEL (1971) Structure of wind-driven equatorial currents in homogeneous oceans. *Journal of Physical Oceanography*, **1**, 149–160.

DU PENHOAT Y. and A. M. TRÉGUIER (1985) The seasonal linear response of the tropical Atlantic Ocean. *Journal of Physical Oceanography*, **15**, 316–329.

ERIKSEN C. C. (1981) Deep currents and their interpretation as equatorial waves in the western Pacific Ocean. *Journal of Physical Oceanography*, **11**, 48–70.

FOFONOFF N. P. and R. B. MONTGOMERY (1955) The Equatorial Undercurrent in the light of the vorticity equation. *Tellus*, **7**, 518–521.

GARZOLI S. L. and E. J. KATZ (1983) The forced annual reversal of the Atlantic North Equatorial Countercurrent. *Journal of Physical Oceanography*, **13**, 2082–2090.

GARZOLI S. L. and S. G. H. PHILANDER (1985) Validation of an equatorial Atlantic model using inverted echo sounder data. *Journal of Geophysical Research*, **90**, 9199–9201.

GENT P. R. and J. R. LUYTEN (1985) How much energy propagates vertically in the equatorial oceans? *Journal of Physical Oceanography*, **7**, 997–1007.

HELLERMAN S. and M. ROSENSTEIN (1983) Normal monthly windstress over the world ocean with error estimates. *Journal of Physical Oceanography*, **13**, 1093–1104.

INOUE M and J. J. O'BRIEN (1984) Forecasting model for the onset of a major El Niño. *Monthly Weather Review*, **112**, 2326–2337.

KATZ E. J. (1984) Basin wide thermocline displacements along the equator off the Atlantic in 1983. *Geophysical Research Letters*, **11**, 729–732.

LEVITUS S. (1982) *Climatological Atlas of the World Ocean*. NOAA Professional Paper 13. U.S. Government Printing Office, Washington, D.C., 173 pp., 17 microfiche.

LUYTEN J. and J. SWALLOW (1976) Equatorial undercurrents. *Deep-Sea Research*, **23**. 1005–1007.

PACANOWSKI R. and S. G. H. PHILANDER (1981) Parameterization of vertical mixing in numerical models of tropical oceans. *Journal of Physical Oceanography*, **11**, 1443–1451.

PHILANDER S. G. H. (1979) Nonlinear equatorial and coastal jets. *Journal of Physical Oceanography*, **9**, 739–747.

PHILANDER S. G. H. and R. C. PACANOWSKI (1986) A model of the seasonal cycle of the tropical Atlantic Ocean. *Journal of Geophysical Research*, in press.

RICHARDSON P. and S. G. H. PHILANDER (1986) Variability of surface currents in the tropical Atlantic Ocean: Ship-drift data and results from a model compared. *Journal of Geophysical Research*, in press.

ROBINSON A. R. (1966) An investigation into the wind as the casue of the Equatorial Undercurrent. *Journal of Marine Research*, **24**, 179–204.

SCHOPF P. S. and M. A. CANE (1983) On equatorial dynamics, mixed layer physics and sea surface temperature. *Journal of Physical Oceanography*, **13**, 917–935.